

Structure Explication, Biological Evaluation, DNA Interaction, Electrochemistry and Antioxidant Activity of Iron (II) tri- and Tetra-Dentate Schiff base Amino Acid Complexes

Ahmed M. Abu-Dief*, Laila H. Abdel-Rahman, Emad F. Newair and Nahla Ali Hashem

Chemistry Department, Faculty of Science, Sohag University, Sohag 82534, Egypt.

Received: 7 Jan. 2021, Revised: 2 Apr. 2021, Accepted: 17 Apr. 2021.

Published online: 1 May 2021

Abstract: New azomethine Schiff base amino acid ligands derived from the condensation reaction of 3-methoxysalicylaldehyde (MS) or 4-diethylaminosalicylaldehyde (DS) with some of α -amino acids (L-phenylalanine (Phe), L-histidine (His), DL-tryptophan (Trp)) and their Fe(II) complexes were prepared. Structures of the synthesized Fe(II) complexes were determined on the basis of elemental analysis, infrared, ultraviolet-visible spectra, thermal analysis and cyclic voltammetry (CV) as well as conductivity, magnetic susceptibility measurements. Moreover, the particle size distribution of the prepared complexes was determined by using transmittance electron microscope (TEM). The experimental results show that the investigated Fe(II) complexes contain hydrated water molecules (except DSPFe complex) and coordinated water molecules (only in MSHFe complex). The kinetic and thermal parameters were determined from the thermal data using Coast and Redfern method. The results suggest that MS or DS amino acid Schiff bases behave as monobasic tridentate ONO ligands and coordinate to Fe(II) in octahedral geometry according to the general formula $[\text{Fe}(\text{HL})_2] \cdot n\text{H}_2\text{O}$. But in the case of MSHFe complex, MSH ligand acts as tetradentate $(\text{NH}_4^+)[\text{Fe}(\text{HL})(\text{H}_2\text{O})\text{SO}_4] \cdot 2\text{H}_2\text{O}$. The conductivity values between $43.30\text{--}5.66 \Omega^{-1} \text{mol}^{-1} \text{cm}^{-2}$ in DMF suggest the presence of non-electrolyte species, except MSHFe complex is electrolyte species ($60.3 \Omega^{-1} \text{mol}^{-1} \text{cm}^{-2}$). Moreover, the antimicrobial evaluation of the prepared Schiff base amino acid ligands and their Fe(II) complexes was examined against three types of bacteria such as *B. subtilis* (+ve), *E. coli* (-ve) and *M. luteus* (+ve) and three types of fungi such as *A. niger*, *C. glabrata* and *S. cerevisiae*. The results of these studies signaling that the metal chelates exhibit a stronger antimicrobial efficiency than their corresponding ligands. Moreover, the interaction of the prepared Fe(II) complexes with (CT-DNA) by using spectral studies, viscosity measurements and agarose gel electrophoresis was investigated. Furthermore, antioxidant activities of the synthesized complexes were examined by using the ABTS assay and showed that the prepared complexes have a good antioxidant activity.

Keywords: Amino acid, Fe(II) complexes, Antimicrobial, Cyclic voltammetry, antioxidant, DNA interaction.

1 Introduction

There are few amino acids which are principles for human beings such as: phenylalanine, tryptophan, and histidine. They are very much necessity, as they cannot be biosynthesized by our body. Phenylalanine: Helps in boosting memory power and helps to maintain a healthy nervous system. Tryptophan: Plays a vital role in maintaining our appetite. Histidine: Helps in the yielding and synthesis of both RBC (red blood cells) and WBC (white blood cells).

Phenylalanine is important in the construction of

structural proteins in tissue. The concentrations of phenylalanine govern the amounts of other electrically neutral amino acids in the brain. Tryptophan catabolism in cancer is progressively more being identified as a marked microenvironmental factor that curbs antitumor immune responses. It has been suggested that the fundamental amino acid tryptophan is catabolized in the tumor tissue by the rate-restrictive enzyme indole amine-2, 3-dioxygenase (IDO) revealed in tumor cells or antigen-presenting cells [1]. Tryptophan is the only amino acid bound to plasma albumin [2]. Part of the tryptophan bound to albumin is available for uptake into the brain

* Corresponding author E-mail: ahmed_benzoic@yahoo.com

[3]. Histidine has numerous therapeutic uses, and it is basically exploited to amplify as well as maintain the healthy tissues in all the body parts. In addition, this amino acid is also used to verify that the messages transported from the brain to different parts of our body reach properly.

The azomethine linkage in Schiff bases is chief of the biological activities such as antitumor, antimicrobial, and herbicidal activities [4]. Some drugs show increased activity when supervised as metal chelates and cramp the growing of tumors [5]. Metal Schiff base complexes have been well published for their easy synthesis, stability, and wide application [6-8]. Schiff bases are generally bi- or tridentate ligands appropriate for forming very stable complexes with transition metals. Studying the interaction between transition metal complexes and DNA has engaged many interests due to their importance in cancer therapy, design of new classes of pharmaceutical molecules and molecular biology [9-13]. Metal complexes of Schiff base phenolates with favorable cell membrane permeability have been capitalized on cancer multidrug resistance and used as antimalarial agents [14].

2 Materials and method

All chemicals used in the preparation of these complexes such as 3-methoxysalicylaldehyde ($C_8H_8O_3$) (MS), 4-diethylaminosalicylaldehyde ($C_{11}H_{15}O_2N$) (DS), amino acids [L-Phenylalanine (Phe), DL-Tryptophan (Trp), L-Histidine (His)], the metal salt [ferrous ammonium sulfate salt ($Fe(SO_4)_2(NH_4)_6 \cdot 6H_2O$)], Calf thymus DNA (CT-DNA), ethidium bromide (3, 8-diamino-5-ethyl-6-phenylphenanthridinium bromide (EB)), Tris [hydroxymethyl] amino methane (2-amino-2-hydroxymethyl-propane-1, 3-diol) (Tris), NaCl, EDTA, TBE buffer, bromophenol blue, ammonium peroxydisulfate solution, ABTS solution, phosphate buffer (pH = 7.4), NiL4 and Trolox solution were obtained from Sigma-Aldrich. Ethanol and dimethyl formamide (DMF) products of spectroscopic grade were used.

1H NMR and ^{13}C NMR spectral measurements were reported on a BRUKER, using DMSO as an internal reference. Melting points for the isolated ligands and decomposition temperatures for their complexes were screened on a melting point apparatus, Cimarec 3 Thermolque. The carbon, hydrogen and nitrogen contents were monitored on a Perkin Elmer (2400) CHNS analyzer. IR spectra (4000–400 cm^{-1}) were enrollment on Shimadzu FT-IR model 8101 spectrometer using KBr pellets. The UV-Vis spectra were recorded on a PG spectrophotometer model T+80 at 298 K. The TG/DT analyses were recorded on a Shimadzu corporation 60 H at 10 degrees min^{-1} . Molar conductance was measured on an Elico CM-180 conductometer at 298 K using DMF as a solvent. Magnetic susceptibility mensuration of the metal complexes were determined by using Gouy balance at room temperature and $Hg[Co(SCN)_4]$ as a calibrant. A

HANNA 211 pH meter at 298 K which used for pH measurements calibrated against standard buffers (pH 4.02 and 9.18) before measurements. TEM measurements were performed on TEM 2100 instrument, the calculated histograms were performed using image J for TEM program (Broken symmetry software). The cyclic voltammetry experiments of the complexes were investigated using an AutolabPGSTAT128N Potentiostat/Galvanostat (Metrohm Autolab B.V., Utrecht, The Netherlands) electrochemical analyzer operated via NOVA software (Metrohm Autolab B.V., Utrecht, The Netherlands).

A predictable three-electrode electrolytic cell was employed, in which glassy carbon electrode; GCE was employed as a working electrode. A platinum electrode and a silver-silver chloride electrode ($Ag/AgCl$ 3.5 M) were used as the counter and reference electrodes; reciprocally antimicrobial evaluation was executed using agar well diffusion. Interaction of the prepared compounds with DNA by using i) absorption spectra were determined by using a UV-Vis spectrophotometer model JASCO V-580 with 1cm quartz cells associated with an ultrathermostate (CRIOTERM model 190) water circulator. Electronic absorption spectrum of the complex was reported before and after addition of CT-DNA in the existence of Tris-HCl buffer (pH 7.2), ii) viscosity measurements were performed by using Ostwald viscometer immersed in a thermostatic water-bath maintained at 25 $^{\circ}C$ and iii) agarose gel electrophoresis was visualized under UV a transilluminator and picked up with a Panasonic DMC-LZ5 Lumix Digital Camera.

2.1 Schiff bases formation method

Schiff base amino acid ligands were prepared (5 mmol, 0.760 g, 0.995 g respectively) of the MS or DS was dissolved in 40 ml ethanol and then added to the solution of the amino acid (5 mmol, 0.825 g, 1.045 g, 1.020 g) (L-Phenylalanine (Phe), DL-Tryptophan (Trp) and L-Histidine (His), respectively) in aqueous-ethanol mixture. The mixture then refluxed for 2 hr; the solvent was removed on suction at room temperature. After a day, yellow powders in case of MS were obtained while brown powders in case of DS were obtained [15].

2.2 Complexes formation method

Aqueous solutions of the amino acids were prepared by dissolving (5 mmol, 0.825 g, 1.045 g, 1.02 g respectively) of each (Phe, Trp, His) in 40 ml of aqueous-ethanol mixture. Each of the solutions was mixed with MS (5 mmol, 0.76 g) or DS (5 mmol, 0.995 g) dissolved in aqueous-ethanol mixture (50 ml). Then the mixture was stirred at 70 $^{\circ}C$ for 1 hr. The obtained ligands solution was treated with an aqueous-ethanol mixture solution (40 ml) of the salt of Fe(II) ($Fe(NH_4)_2(SO_4)_2 \cdot 6H_2O$) (2.5 mmol, 0.98 g)(5 mmol, 1.96 g in the case of MSHFe complex). In order to void oxidation of Fe (II), we added a few drops of glacial acetic acid. Then the mixture was stirred at room temperature for 3 hr. The obtained

products were evaporated overnight. The obtained solid products were filtered, washed with water and dried in ver anhydrous CaCl_2 [16].

2.3 Kinetic data for TGA of the prepared complexes

The activation parameters of thermodynamic of decomposition processes of complexes namely activation energy, enthalpy, entropy and Gibbs free energy change of the disintegration (E^* , H^* , S^* , G^* respectively) were evaluated graphically by employing the Coats-Redfern relation [17].

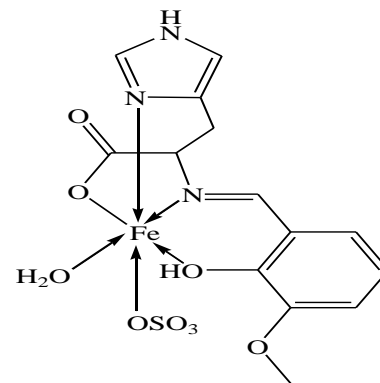
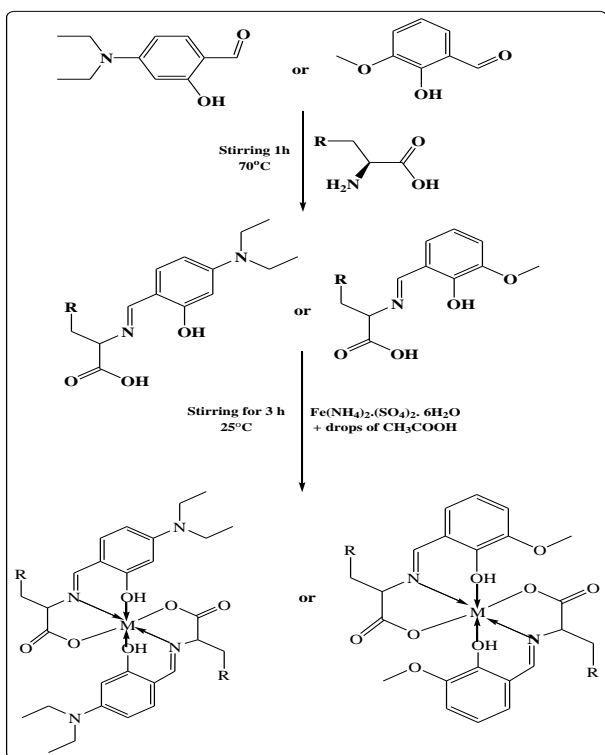
$$\text{Log}\left[\frac{\log\{W_\infty/(W_\infty-W)\}}{T^2}\right] = \text{log}\left[\frac{AR}{(\phi E^*)}\left(1-\frac{2RT}{E^*}\right)\right] - \frac{E^*}{2.303RT} \quad (1)$$

Where W_∞ , W , R and ϕ are the mass loss at the completion the decomposition reaction, the mass loss up to temperature T , the gas constant and the heating rate of the decomposition, respectively; Since $1-2RT/E^* \sim 1$, the plot of the left-hand side of equation (1) versus $1/T$ would give straight line. E^* was then calculated from the slope and from the intercept we obtained the Arrhenius constant (A).

The other kinetic parameters: S^* , H^* and G^* were calculated using the following equation:

- (2) $S^* = 2.303 R \log Ah/(K_B T)$
- (3) $H^* = E^* - RT$
- (4) $G^* = H^* - TS^*$

Where, (KB) and (h) are the Boltzmann's and Planck's constant, respectively.



Scheme (1): The proposed structures of MSHFe complex

2.4. Antimicrobial bioassay

The newly synthesized Schiff base amino acid ligands and their complexes were screened against two Gram-positive (*B. subtilis* and *M. luteus*) and one Gram-negative (*E. coli*) by well diffusion method [18] using agar nutrient. The antifungal activities were tested against three types of fungi: *A. niger*, *C. glabrata* and *S. cerevisiae* by well diffusion method. Ciprofloxacin and Amphotericin B are used as control for bacteria and fungi, respectively. The suspension of per microorganism was added to a sterile agar medium, then gushed into sterile Petri plates and left to solidification. The test solution of the prepared complexes (15, 30 mg/ml) was prepared by dissolving the compounds in DMSO and the well was replete with the test solution of the prepared complexes using micropipette. The plates were incubated for 24 hr for bacteria and 72 hr for fungi at 35 °C. The extracts were subjected to further assay with a series on time basis (24, 48 and 72 hr). During this period, the test solution of the prepared complexes was prevailed and affected the growth of the inoculated microorganisms. Determination of activity by measuring the zone diameter (mm), growth of repression was emulated with the control.

2.5 Interaction with Calf Thymus DNA (CT-DNA)

By using absorption spectral studies, Absorption titrations were completed by keeping the concentration of the complex constant and by varying the concentration of CT-DNA from 3 to 30 μM . The interaction of the complexes with DNA was carried out in Tris-HCl buffer (10 μM , pH 7.2). The Tris-HCl buffer solution was prepared using de ionized water and was used to control the pH of the reaction system. The binding constant K_b for the binding of the complexes with DNA, have been decided from the spectroscopic titration data using the subsidiary equation [19]:

$$[\text{DNA}]/(\epsilon_a - \epsilon_f) = [\text{DNA}]/(\epsilon_b - \epsilon_f) + 1/K_b(\epsilon_b - \epsilon_f) \quad (5)$$

Where $[\text{DNA}]$ is the concentration per nucleotide, the

apparent extinction coefficient ϵ_a was obtained by $A_{obs}/[complex]$. The ϵ_f is the extinction coefficient of the complex in the presence of DNA and ϵ_b is the extinction coefficient for the ternary complexes in the fully bound form. The data were suited to the above equation with a slope equal to $1 / (\epsilon_b - \epsilon_f)$ and intercept equal to $1 / [K_b (\epsilon_b - \epsilon_f)]$ and K_b was acquired from the ratio of the slope to the intercept, obtained from a plot of $[DNA] / (\epsilon_a - \epsilon_f) [DNA]$. The standard Gibbs free energy for DNA binding was tabulated from the following relation.

$$\Delta G^{\circ}_b = -RT \ln K_b \quad (6)$$

Where R , T and K_b are the general gas constant, the absolute temperature and the binding constant respectively

By using viscosity measurements, viscosity examination were achieved in an Ostwald viscometer maintained at 25 °C in a thermostatic water-bath, to shrink complexities originating from DNA flexibility. The flow times of the samples were determined with a digital stopwatch organized timer for different concentrations of the complex (10–250 μ M), preserving the concentration of DNA constant (250 μ M). The control sample was carried out on ethidium bromide (EB) by utilizing the same method. The buffer influx time was registered as t_0 . Data accessed were given as $(\eta/\eta_0)^{1/3}$ vs $1/R$ ($R = [DNA]/[Complex]$), where η and η_0 are the viscosity of DNA in presence of complexes and the viscosity of DNA alone respectively. Viscosity values were calculated from the examined flow time of DNA-containing solution corrected for flux time of buffer alone (t_0), $\eta = t - t_0 / t_0$ [20].

By using agarose gel electrophoresis, the gel is prepared by dissolving the agarose powder in an appropriate buffer, such as TBE (45 μ M Tris, 45 μ M boric acid and 1 μ M EDTA, pH 7.3), to be used in electrophoresis [21]. The agarose is distributed in the buffer before heating it to near-boiling point, but obviate boiling. The melted agarose is permitted to cool satisfactorily before flooding the solution into a cast as the cast may crack if the agarose solution is too hot. A comb is putted in the cast to establish wells for loading sample, and the gel should be completely installed before use. For a standard agarose gel electrophoresis, 1 % gels are common for many applications [22]. Once the gel has set, the comb is eliminated, departure wells where DNA samples can be stuffed. Loading buffer is mixed with the DNA sample and synthesized complex. The loading buffer also contains colored dyes such as bromophenol blue used to monitor the evolution of the electrophoresis. The DNA samples are loaded using a pipette. The buffer used in the gel is the same as the procession buffer in the electrophoresis container, which is why electrophoresis in the submarine mode is possible with agarose gel. Since DNA is not visible in natural light, the development of the electrophoresis is monitored using colored dyes. Bromophenol blue (dark blue) comigrates with the

smaller fragments. A DNA marker is also run together for the appreciation of the molecular weight of the DNA fragments. DNA is normally visualized by staining with ethidium bromide, which intercalates into the dominant grooves of the DNA and fluoresces under UV light. The ethidium bromide may be supplement to the agarose solution before it gels. When stained with ethidium bromide, the gel is viewed with an ultraviolet (UV) transilluminator. These transilluminator apparatus may also accommodate image capture devices, such as a digital or Polaroid camera that permit an image of the gel to be taken or printed.

2.6. Antioxidant activities of the prepared complexes by using ABTS method

The synthesized complexes were investigated by the ABTS assay. The ABTS assay is based on the scavenging ability of antioxidants to the long-life $ABTS^{\cdot+}$ radical cation [23]. A stock solution of the $ABTS^{\cdot+}$ radical cation was generated chemically by mixing of ammonium peroxodisulfate solution (0.2 ml, 65 $mmol\ dm^{-3}$) with 50 ml of ABTS solution (1 $mmol\ dm^{-3}$, work out in 0.1 $mol\ dm^{-3}$ phosphate buffer pH 7.4). The mixture was left overnight and then 0.5 ml of $ABTS^{\cdot+}$ radical cation stock solution was mixed with phosphate buffer (2 ml) (pH 7.4) in a cuvette and the absorbance at 734 nm (A_{ABTS}) was measured. Subsequently, 0.5 ml of 0.5 $mmol\ dm^{-3}$ NiL4 was added in the cuvette, the solution was mixed quickly, and the absorbance at 734 nm ($A_{complex}$) was respected after 60 s. The decrease in absorbance ($\Delta A = A_{ABTS} - A_{complex}$) after 60 s was calculated. The decrease in absorbance caused by the addition of Trolox as the standard was measured by the same procedure for each concentration of Trolox (50–600 μ mol/L) and the calibration curve for the decrease in absorbance ($\Delta A = A_{ABTS} - A_{Trolox}$) of Trolox vs. Trolox concentration was constructed by linear regression.

3 Results and Discussion

3.1. Characterization of the prepared compounds

3.1.1. 1H NMR and ^{13}C NMR spectra of the prepared Schiff base amino acid ligands

The 1H NMR spectrum (DMSO- d_6 , ppm) of MSP, MST and MSH ligands show singlet signal at 13.6, 13.6 and 13.4 for COOH proton respectively, singlet signal at 8.4, 8.2 and 8.9 for CH=N proton respectively, multiple signals at 7.4 – 6.6 for eight, nine and five aromatic protons respectively. Also, they show singlet signal at 4.3, 4.3 and 4.8 for OH proton respectively, singlet signal at 3.9, 3.7 and 3.8 for CH aliphatic proton respectively and singlet signal at 3.8, 3.8 and 3.7 for three OCH_3 protons respectively. Furthermore, they show doublet signals at 3.2, 3.0 and 3.0 for three CH_2 protons appropriately and

the ¹H NMR spectrum of MST and MSH ligands showed singlet signal at 10.9 and 11.0 for NH proton respectively. The ¹H NMR spectrum of DSP, DST and DSH ligands show singlet signal at 11.0, 11.6 and 11.5 for COOH proton respectively, singlet signal at 8.5, 8.1 and 8.3 for CH=N proton respectively, multiple signals at 7.4 – 6.1, 7.5–6.8 and 7.5– 6.0 for five, eight and eight aromatic protons respectively. Also, they show singlet signal at 5.0, 4.2 and 4.3 for OH proton respectively, singlet signal at 3.4, 3.2 and 3.5 for CH aliphatic proton respectively and quartet signals at 3.4, 3.5 and 3.3 for four (2 CH₂-CH₃) protons respectively. Furthermore, they show triplet signals at 1.1, 1.2 and 0.9-1.2 for six (2 CH₃-CH₂) protons respectively and the ¹H NMR spectrum of DST and DSH ligands showed singlet signals at 10.7 and 9.5 for NH proton respectively.

¹³C NMR spectrum of MSP, MST and MSH ligands are displaying the signals conforming to the different non-equivalent carbon atoms at different values of δ as follows : at δ 193, 171 and 177 ppm (COOH) due to carboxylic acid group in the amino acid respectively, at δ 171, 168 and 170 ppm (CH=N) due to azomethine respectively and at δ 151-118, 165-70 and 150-115 ppm (12 CH – Ar), (14 CH – Ar) and (9 CH – Ar) due to aromatic carbon atoms respectively. Also, at δ 71, 58 and 56 ppm (OCH₃) due to carbon atom of methoxy group respectively, at δ 55, 52 and 62 ppm (CH) due to aliphatic carbon atom respectively and at δ 41, 29 and 33 ppm (CH₂) agreeing to the carbon atom in methyl group respectively.

¹³C NMR spectrum signals of DSP, DST and DSH ligands are displaying at δ 191, 194 and 197 ppm (COOH) due to carboxylic acid group in the amino acid respectively, at δ 165, 163 and 163 ppm (CH=N) due to azomethine and at δ 163- 99, 148–100 and 158–100 ppm (12 CH – Ar), (14 CH – Ar) and (9 CH – Ar) due to aromatic carbon atoms respectively. Also, at δ 50, 53 and 52 ppm (CH) due to aliphatic carbon atom respectively, at δ 40, 38 and 38 ppm (CH₂-N) corresponding to carbon atom in diethyl group respectively and at δ 39, 36 and 35 ppm (CH₂-Ar) corresponding to carbon atom connected with aromatic group respectively. Furthermore, at δ 17, 13 and 13 ppm (CH₃) due to carbon atom in diethyl group respectively.

3.1.2. Microanalysis, conductivity and magnetic moment measurements

The microanalysis results suggest that MS or DS amino acid Schiff bases behave as monobasic tridentate ONO ligands and coordinate to the metal in octahedral geometry according to the general formula [Fe(HL)₂].nH₂O. But in the case of MSHFe complex, the MSH ligand acts as tetradentate ((NH₄⁺)[Fe(HL)(H₂O)SO₄].2H₂O). The molar conductivity measurements were carried out in DMF. The molar conductance values in Table 1. The conductivity

values of prepared MSPFe, MSTFe, MSHFe, DSPFe, DSTFe and DSHFe complexes are 30.8, 32.5, 60.3, 25.8, 53.3 and 5.7 $\Omega^{-1} \text{ mol}^{-1} \text{ cm}^{-2}$ respectively, in DMF imply the presence of non-electrolyte species, except MSHFe complex is electrolyte species (60.3 $\Omega^{-1} \text{ mol}^{-1} \text{ cm}^{-2}$). Magnetic susceptibility measurements Table 1 values of the synthesized MSPFe, MSTFe, MSHFe, DSPFe, DSTFe and DSHFe complexes are 5.4, 4.9, 4.6, 4.8, 5.2 and 5.5 B. M respectively which suggests octahedral geometry of the complexes.

3.1.3. Infrared spectra

Infrared spectrum refers to the part of the electromagnetic spectrum between amidst the visible and microwave regions. Infrared spectroscopy utilizes the fact that molecules devour specific frequencies that are characteristic of their structure. IR spectroscopy is often accustomed detect structures because functional groups give rise to characteristic bands both in terms of intensity and position (frequency). The important infrared spectral bands and their assignments for the synthesized ligands and their complexes were taped as KBr pellets and were presented in Table 2. The IR data of the free ligands and their complexes were achieved within the IR range 4000-400 cm^{-1} . The IR spectrum of the free Schiff base amino acid ligands show a broad band around 3441-3389 cm^{-1} , which is assigned to the stretching frequency of the aromatic hydroxyl substituent group, troubled by intramolecular hydrogen bonding [O—H—N] between phenolic hydrogen and azomethine nitrogen atoms [24, 26]. Further, the appearance of the OH band around 3499-3399 cm^{-1} in the spectra of the complexes with an enlargement intensity signalizes that the hydroxyl oxygen is coordinated to the M(II) ion without proton displacement [27]. Due to azomethine $\nu(\text{C}=\text{N})$ linkage appeared in all the ligands and their Fe(II) complexes [28, 29] indicating that the condensation between ketone moiety of aldehyde and that of amino group of amino acid has taken place resulting into the formation of the desired ligands. Moreover, on comparison of the IR spectra of the Schiff base amino acid ligands with their Fe(II) complexes showed a major shift to lower wave numbers by 20 - 43 cm^{-1} in azomethine $\nu(\text{C}=\text{N})$ suggesting the involvement of the azomethine nitrogen with the Fe(II) ion [30, 31]. These facts suggest coordination of the ligand with the metal atom via the azomethine nitrogen and phenolic oxygen. The $\nu(\text{C} - \text{O})$ (phenolic) vibration of ligands are observed around 1235-1293 cm^{-1} , which gets shifted to lower or higher frequency region in the complexes indicating coordination of phenolic oxygen [32]. The ligands exhibit other two intense bands at (1362-1443), (1572-1599) cm^{-1} corresponding to symmetric (S) and asymmetric (As) stretching frequencies of (COOH) group, respectively of the organic ligand. On complexation symmetric and asymmetric bands were

transmitted to a lower frequency [33]. $\Delta \nu$ (COO⁻) \sim 200 cm⁻¹ indicated the unidenticality of the carboxylate group [34]. This reality is also supported by the appearance of non-ligand bands at appropriate positions in the far infrared region (700-739 cm⁻¹ and 524-562 cm⁻¹) due to ν

(Fe-N) and ν (Fe-O) vibrations, respectively [35-38]. Furthermore, the peaks found at 1074 cm⁻¹ are assigned to the bending vibration of the coordinated sulfate (OSO₃²⁻) in MSHFe complex [39].

Table 1: Analytical and physical data of Schiff base amino acid ligands and their complexes

Comp.	Molecular formula (M. Wt)	μ_{eff} (B.M)	Λ_m , Ohm ⁻¹ cm ² mol ⁻¹	M. p. and Decomp. (°C)	Elemental Analysis found (calc.) %		
					C	H	N
MSP	C ₁₇ H ₁₇ NO ₄ (299.0)		14.9	220	67.70 (67.73)	5.62 (5.68)	4.50 (4.58)
MSPFe	C ₃₄ H ₃₆ O ₁₀ N ₂ Fe (688)	5.4	30.8	285	59.30 (59.37)	4.60 (4.66)	4.17 (4.20)
MST	C ₁₉ H ₁₈ N ₂ O ₄ (338.0)		20.5	240	67.28 (67.31)	5.10 (5.22)	8.05 (8.18)
MSTFe	C ₃₈ H ₃₈ O ₁₀ N ₄ Fe (766)	4.8	32.5	>300	59.53 (59.62)	4.43 (4.50)	7.31 (7.39)
MSH	C ₁₄ H ₁₅ N ₃ O ₄ (289)		12.4	240	58.13 (58.20)	5.19 (5.24)	14.53 (14.60)
MSHFe	C ₁₄ H ₂₄ O ₁₁ N ₄ SFe (512)	4.6	60.3	>300	32.81 (32.89)	5.08 (5.12)	10.94 (11.02)
DSP	C ₂₀ H ₂₄ N ₂ O ₃ (340.0)		8.2	160	70.40 (70.52)	6.98 (7.06)	8.11 (8.23)
DSPFe	C ₄₀ H ₄₆ O ₆ N ₄ Fe (734)	4.8	25.8	>300	65.40 (65.48)	6.02 (6.10)	7.31 (7.52)
DST	C ₂₂ H ₂₅ N ₃ O ₃ (379.0)		6.6	200	69.58 (69.66)	6.52 (6.60)	10.97 (11.08)
DSTFe	C ₄₄ H ₅₈ O ₁₁ N ₆ Fe (902)	5.2	43.3	280	58.40 (58.51)	6.32 (6.41)	9.91 (9.97)
DSH	C ₁₇ H ₂₂ N ₄ O ₃ (330)		19.4	275	61.82 (61.91)	6.67 (6.72)	16.97 (17.02)
DSHFe	C ₃₄ H ₄₄ O ₇ N ₈ Fe (732)	5.5	5.7	300	55.74 (55.81)	6.88 (6.91)	15.28 (15.32)

Table 2: IR spectral data of the investigated Schiff base amino acid ligands and their complexes.

Comp.	ν (OH)/H ₂ O	ν_{St} (-C=N)	ν_{As} (COO)	ν_{S} (COO)	ν (Fe-N)	ν (Fe-O)
MSP	3438 (m)	1634 (s)	1589 (m)	1410 (m)	-	-
MSPFe	3489 (s)	1614 (s)	1548 (w)	1387 (w)	736 (s)	562 (w)
MST	3389 (m)	1651 (s)	1588 (w)	1362 (m)	-	-
MSTFe	3399 (s)	1613 (s)	1549 (w)	1343 (w)	737 (s)	551 (w)
MSH	3399 (m)	1636 (s)	1577 (w)	1386 (m)	-	-
MSHFe	3428 (s)	1614 (s)	1549 (w)	1361 (m)	739 (m)	539 (m)
DSP	3441 (m)	1632 (s)	1573 (s)	1405 (s)	-	-
DSPFe	3489 (s)	1608 (s)	1517 (m)	1339 (m)	700 (m)	525 (w)
DST	3414 (m)	1628 (s)	1599 (m)	1443 (m)	-	-
DSTFe	3428 (s)	1585 (s)	1516 (m)	1338 (m)	704 (m)	525 (w)
DSH	3438 (m)	1640 (s)	1572 (w)	1430 (m)	-	-
DSHFe	3496 (s)	1608 (s)	1559 (w)	1415 (w)	701 (s)	524 (m)

3.1.4. Electronic spectra

Electron spectroscopy is an analytical approach to investigate the electronic structure and its dynamics in atoms and molecules. The electronic spectra of all the complexes in DMF showed in Figure 1.

The electronic spectra of all the Schiff base amino acid ligands showed two types of transitions, the first one appeared at below 300 nm which can be assigned to π - π^* transition due to transitions including molecular orbitals located on the phenolic and carboxylic chromophore. This reveals that the coordination site is oxygen of the phenolic

and carboxylic groups.

The second type of transitions appeared at range 315-457 nm assigned to $n \rightarrow \pi^*$ transition due to azomethine groups and benzene ring of the ligands. These bands have also been moved in the spectra of the new complexes indicating the involvement of imine group nitrogen's in coordination with central metal atom.

Moreover, there is a band shown in the region 413-331 nm, assigned to ligand-to-metal charge transfer (LMCT) [40]. A broad band from 486- 523 nm, which mark that band could be mainly referred to $d \rightarrow d$ transition in an octahedral structure of the prepared complexes [16, 41].

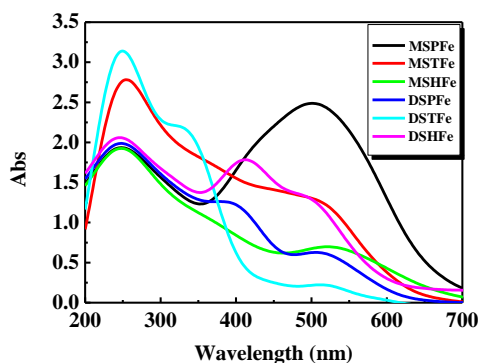


Fig. 1: Molecular electronic spectra of $[DSHFe] = [DSTFe] = [DSPFe] = 2 \times 10^{-4} \text{ mol dm}^{-3}$, $[MSTFe] = 3 \times 10^{-4} \text{ mol dm}^{-3}$, $[MSPFe] = [MSHFe] = 1 \times 10^{-3} \text{ mol dm}^{-3}$.

3.1.5. Determination of stoichiometry of and formation constant of the synthesized complexes

The stoichiometry of the prepared complexes formed in solutions via the reaction of metal with the studied Schiff base amino acid Schiff base ligands was established by using continuous variation technique as shown in Figure 2. Complexes of Fe(II) with metal ions were studied in solution by help of ethanol as a solvent, in order to establish $[M: L]$ mole ratio in the complex follow molar ratio method [42]. A series of solutions were prepared having a fixed concentration of the metal ion and the $[M: L]$ ratio was determined from the relationship among the absorption of the absorbed light and the mole ratio of $[M: L]$. In continuous variations method, the total number of moles of reactants is conserved constant for a series of measurements. Each value will occur when the mole ratio of the reactants is coterminous to the optimum ratio which is the stoichiometric ratio in the chemical equation. Maximum in the curve at $X_{\text{ligand}} = 0.62-0.73$ implicates a 1:2 (metal ion to ligand) molecular association.

The formation constants (K_f) of the studied complexes constructed in solution were checked from the spectrophotometric mensuration using the continuous variation method [43].

The obtained formation constants (K_f) values display the high stability of the prepared complexes. The values of K_f for the studied complexes build up in the following order: $MSPFe > DSPFe > DSHFe > DSTFe > MSTFe > MSHFe$ complex. Moreover, the values of the stability constants (pK) and Gibbs free energy (ΔG^\ddagger) of the explored complexes are cited in Table 3. The negative values of ΔG^\ddagger mean that the reaction is spontaneous and favorable. Stability of MSHFe complex is less because the presence of water in the complex.

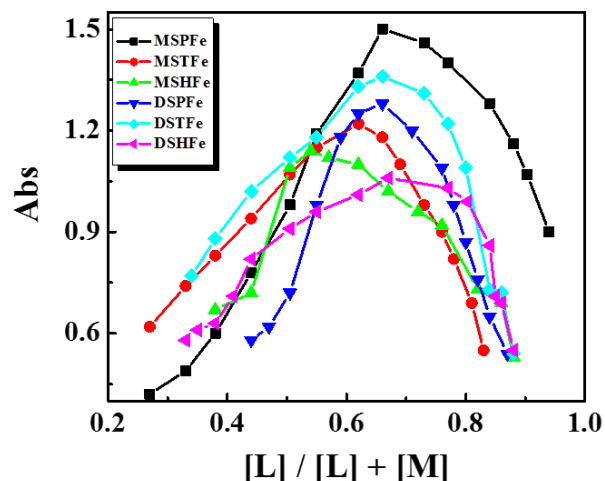


Fig 2: Continuous variation plot for the prepared complexes in aqueous-ethanol mixture at $[Fe^{2+}] = [MSH] = [DST] = 2.1 \times 10^{-3} \text{ mol dm}^{-3}$, $[Fe^{2+}] = [DSH] = 1.4 \times 10^{-3} \text{ mol dm}^{-3}$, $[Fe^{2+}] = [MSP] = 8.0 \times 10^{-3} \text{ mol dm}^{-3}$, $[Fe^{2+}] = [MST] = 1.2 \times 10^{-2} \text{ mol dm}^{-3}$, $[Fe^{2+}] = [DSP] = 3.3 \times 10^{-3} \text{ mol dm}^{-3}$ and 298 K.

Table 3: The formation constants (K_f), stability constants

Complex	Type of complex	K_f	pK	ΔG^\ddagger kJ mol ⁻¹
MSPFe	1: 2	1.6×10^{11}	25.8	-63.9
MSTFe	1: 2	6.9×10^8	20.4	-50.4
MSHFe	1: 1	1.5×10^7	16.5	-40.9
DSPFe	1: 2	1.5×10^{10}	23.4	-57.9
DSTFe	1: 2	9.8×10^8	20.7	-51.3
DSHFe	1: 2	2.6×10^9	23.9	-59.4

(pK) and Gibbs free energy (ΔG^\ddagger) values of the prepared complexes in aqueous - ethanol at 298 K.

3.1.6. Thermogravimetric analyses (TGA) of the prepared complexes

TGA of the synthesized complexes were used to: (i) get information about the thermal stability of these new complexes and (ii) decide whether the water molecules (if present) are inside or outside the inner coordination sphere of the central metal ion. In the present studies, heating rates were suitably controlled at $10 \text{ }^\circ\text{C min}^{-1}$ under nitrogen atmosphere, and the weight losses were

determined from the ambient temperature up to = 750 °C. Thermogram of prepared Fe(II) complexes is observed in three steps, (1) a small weight loss which is assigned to loss of lattice water, (2) maximum weight loss is attributable to the loss of coordinated water, but in this paper, MSHFe complex only contain coordinated water, (3) gradual weight loss can be assigned to complete

decomposition of ligand moiety around the metal ion. Finally, complexes are converted into their metal ion. Table 4 shows the TGA of the prepared complexes.

Table 4: Thermal analysis of the prepared complexes

Complex	Temp. °C	Fragment loss %		Weight loss %	
		Molecular formula	Molecular weight	Found	Calc.
MSPFe	15.7-102.4	2H ₂ O	36	5.20	5.23
	104.1-223.8	C ₉ H ₈ NO ₂	162	23.49	23.55
	225.1-316.5	C ₈ H ₈ O ₂	136	19.67	19.72
Residue	317.8-414.8	C ₁₇ H ₁₆ O ₄ N	298	43.22	43.31
	>750	Fe	56	8.10	8.14
MSTFe	28.3-101.4	2H ₂ O	36	4.62	4.69
	103.4-269.5	C ₉ H ₈ N	130	16.89	16.92
	270.3-442.4	C ₁₁ H ₉ N ₂ O ₂	201	26.21	26.24
	443.6-613.3	C ₁₀ H ₉ NO ₄	207	26.98	27.02
Residue	614.5-750.5	C ₈ H ₈ O ₂	136	17.63	17.67
	>750	Fe	56	7.28	7.31
DSPFe	21.5-238.1	C ₁₁ H ₁₅ NO	177	24.08	24.11
	239.4-343.7	C ₉ H ₈ NO ₂	162	22.05	22.07
	344.9-433.3	C ₇ H ₇	91	12.33	12.39
Residue	434.6-508.9	C ₁₃ N ₂ O ₃ H ₁₆	248	33.69	33.74
	>750	Fe	56	7.59	7.63
DSHFe	34.9-110.7	H ₂ O	18	2.35	2.40
	112.4-314.9	C ₁₁ H ₁₅ NO	177	24.11	24.18
	316.1-420.3	C ₇ H ₆ N ₃ O ₂	152	20.37	22.40
Residue	422.0-503.3	C ₁₇ H ₂₁ N ₄ O ₃	329	44.89	44.92
	>750	Fe	56	7.61	7.65
MSHFe	14.9-144.0	NH ₄ ⁺ +2H ₂ O	54	10.32	10.40
	145.3-274.0	SO ₄ +H ₂ O	114	22.11	22.16
	275.2-385.3	C ₄ H ₅ N ₂	81	15.73	15.81
Residue	386.5-747.2	C ₁₀ NO ₄ H ₉	207	40.22	40.29
	>750	Fe	56	10.82	10.91
DSTFe	27.6-75.3	5H ₂ O	90	9.71	9.77
	76.6-130.3	C ₇ H ₅ O	105	11.58	11.64
	131.6-220.0	C ₄ H ₁₀ N	72	7.34	7.38
	221.7-276.3	C ₄ H ₁₀ N	72	7.91	7.98
	277.5-397.2	C ₉ NH ₈	130	14.38	14.41
	398.5-474.2	C ₉ NO ₃ H ₆	176	19.51	19.58
Residue	475.9-748.3	C ₁₁ N ₂ H ₉ O ₂	201	22.23	22.28
	>750	Fe	56	6.19	6.21

3.1.6.1. Kinetic Data for TGA of the prepared complexes

The data are summarized in Table 5. The value of ΔG^* increases for the subsequently decomposition stages of a given complex. This is due to rising the values of $T\Delta S^*$ from one stage to another. Increasing the values of ΔG^* of a given complex as going from one decomposition step to another indicates that the rate of removal of the sequent ligand will be lower than that of the precedent ligand. This may be attributed to the structural rigidity of the remaining complex after the eviction of one and more

ligands, as compared with the precedent complex, which require more energy, $T\Delta S^*$, for its regulation before undergoing any change. The negative values of activation entropies ΔS^* suggest a more ordered stimulated complex than the reactants and/or the reactions are slow. The positive values of ΔH^* mean that the decomposition procedures are endothermic [44, 45, 46, 47, 48].

3.1.7. Stability range of the synthesized complexes

The stability range of the studied complexes was found to be from [pH = (5-9) for MSPFe, (3-11) for MSHFe, (4-10)

for DSHFe, (3-9) for MSTFe, (6-9) for DSPFe and (4-8) for DSTFe] according to the obtained pH-absorbance curves (Fig. 3). This means that Fe(II) ion greatly stabilizes the tested Schiff base amino acid ligands in this range. Accordingly, these ligands can be utilized as masking reagents of Fe(II) ions in that range of pH [47, 48].

3.1.8. Determination of the particle size distribution for the prepared using TEM

Figs. ((4- 7) (a, b)) shows TEM images of the prepared complexes. TEM images indicate that a sphere-like

structure for the MSHFe, DSPFe and DSTFe complexes which is considered as a self-assembled or agglomerated from nanoparticles structure. The TEM image of MSPFe complex show that this complex has a fiber shape. Moreover, the calculated histogram for the particle size shows that the prepared complexes have 30, 63, 22 and 18 nm for MSPFe, MSHFe, DSPFe, DSTFe complexes, respectively. This concludes that the prepared Schiff base amino acid complexes could have high surface area and could be possessed catalytic activity [47].

Table 5: Thermodynamic data of the thermal decomposition of prepared complexes

Complex	Temp. (°C)	E* KJ/mol	A S ⁻¹	Thermodynamic Parameters		
				ΔS* (J/mol)	ΔH* (KJ/mol)	ΔG* (KJ/mol)
MSPFe	58.2	0.5	0.6	-235.5	-0.5	13.2
	195.1			-245.5	-1.6	46.3
	269.3			-248.2	-2.2	64.6
	377.9			-251.0	-3.1	91.7
MSTFe	53.1	0.4	0.5	-235.9	-0.4	12.1
	195.2			-246.7	-1.6	46.5
	344.7			-251.5	-2.9	83.8
	473.5			-254.1	-3.9	116.4
MSHFe	60.3	0.4	0.4	-238.6	-0.5	13.9
	254.7			-250.5	-2.1	61.7
	296.4			-251.8	-2.5	72.1
	486.1			-255.9	-4.0	120.4
DSPFe	201.9	0.4	0.4	-248.8	-1.7	48.6
	287.9			-251.7	-2.4	70.1
	362.1			-253.7	-3.0	88.9
	492.8			-256.2	-4.1	122.2
DSTFe	53.9	0.5	0.5	-235.7	-0.4	12.3
	95.7			-240.5	-0.8	22.2
	187.7			-246.1	-1.6	44.7
	245.4			-248.3	-2.0	58.9
	345.2			-251.2	-2.9	82.8
	454.7			-253.5	-3.8	111.5
DSHFe	612.1	0.5	0.6	-255.9	-5.1	151.6
	85.7			-239.3	-0.7	19.8
	175.5			-245.2	-1.5	41.6
	268.3			-248.8	-2.2	64.5
	361.4			-251.2	-3.0	87.8
473.7	-153.5	-3.9	116.1			

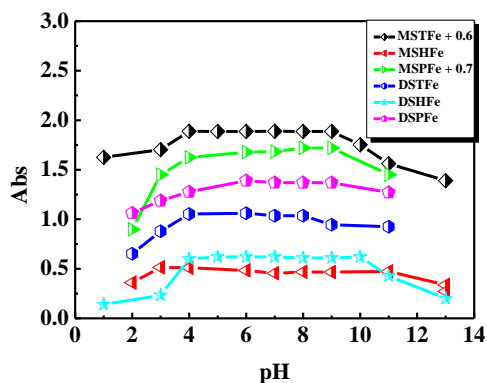


Fig. 3: pH profile of the prepared Schiff base amino acid Fe(II) complexes at [complex] = 1.0×10^{-3} mol dm⁻³ (except [MSTFe] = 7.8×10^{-4} and [DSPFe] = 4.2×10^{-4} mol dm⁻³) and 298 K.

3.1.9. Cyclic voltammetry of the prepared complexes

Fig. 8 explains the cyclic voltammograms of investigated complexes in 0.4 MPBS (pH 6.45) at scan rate 50 mVs⁻¹.

The results of cyclic voltammetry are collected in Table 7. The six complexes demonstrate an oxidative wave positive to reference electrode (Ag/AgCl) in the potential

range 0.0 to 1.6 V. The oxidation wave is assigned to the process of Fe(II) to Fe(III) i.e., the oxidation is primarily metal-centered electron extraction. It is obvious that the oxidation process of the six complexes is irreversible in nature.

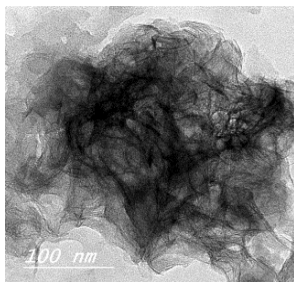


Fig. 4a: TEM image of MSPFe complex.

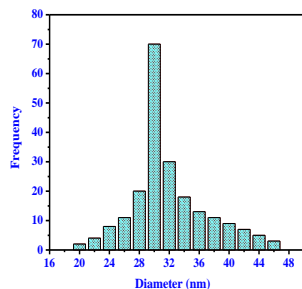


Fig. 4b: Calculated histogram for the particles size distribution of MSPFe complex.

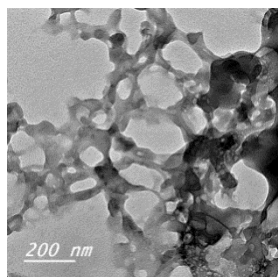


Fig. 5a: TEM image of MSHFe complex

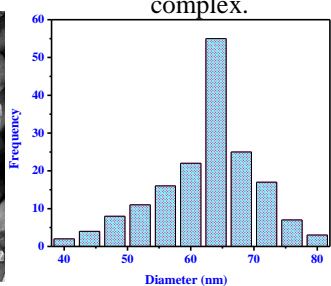


Fig. 5b: Calculated histogram for the particles size distribution of MSHFe complex.

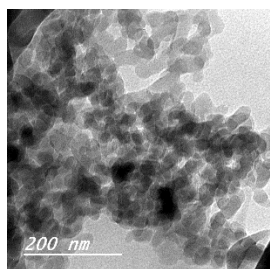


Fig. 6a: TEM image of DSPFe complex

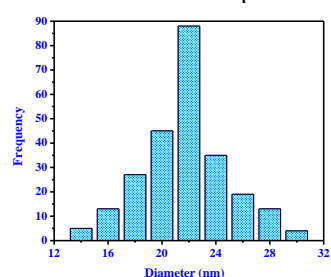


Fig. 6b: Calculated histogram for the particles size distribution of DSPFe complex.

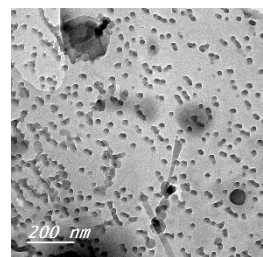


Fig. 7a: TEM image of DSTFe complex

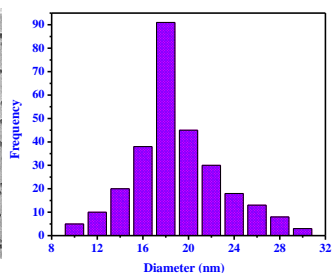


Fig. 7b: Calculated histogram for the particles size distribution of DSTFe complex.

3.2. Biological importance of the prepared complexes

3.2.1. Antimicrobial studies

The main target of the production and synthesis of any antimicrobial compound is to control the causal microbe without any side effects on the patients. The results show that all compounds exhibit antibacterial activity, inhibition properties of the prepared complexes is higher than the free ligands. This may be due to the change in structure due to coordination and chelating trends to make metal complexes act as more powerful and potent bacteriostatic agents, thus inhibiting the growth of the microorganisms. Moreover, coordination decreases the polarity of the metal ion mainly because of the partial sharing of its positive charge with the donor groups within the chelate ring system created through the coordination. This would suggest that the chelation could facilitate the capability of a complex to cross a cell membrane and can be explained by Tweedy's chelation theory [49]. A comparison of the biological activity of the prepared Schiff base amino acid ligands and their complexes with some known antibiotics (Ciprofloxacin and Amphotericin B) is presented and Figs. 9, 10. Some of the prepared Schiff base amino acid complexes were as effective as the antibiotics mentioned. Due to these results, we can be able to use these complexes as antibiotic.

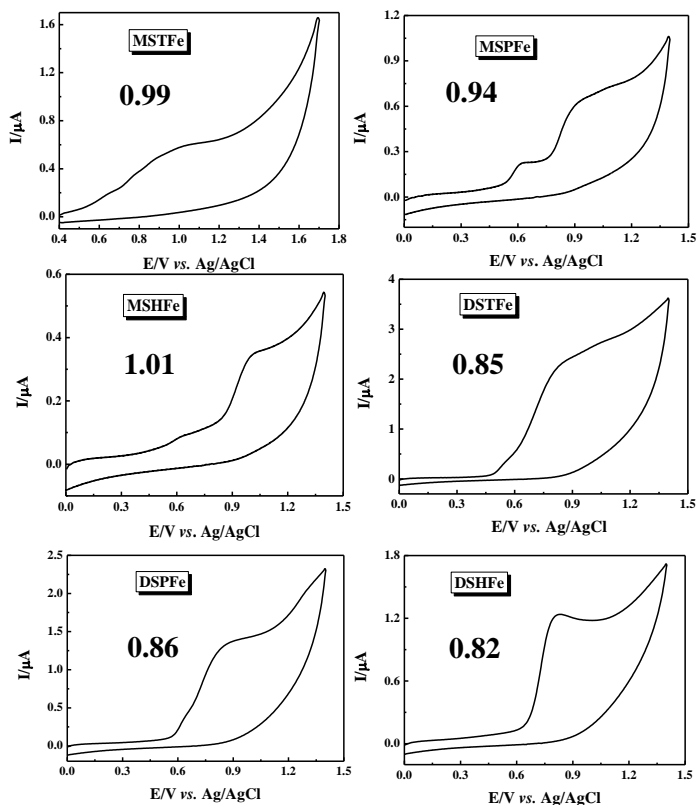


Fig. 8: CV spectra of 25 μM complexes at scan rate 50 mVs^{-1}

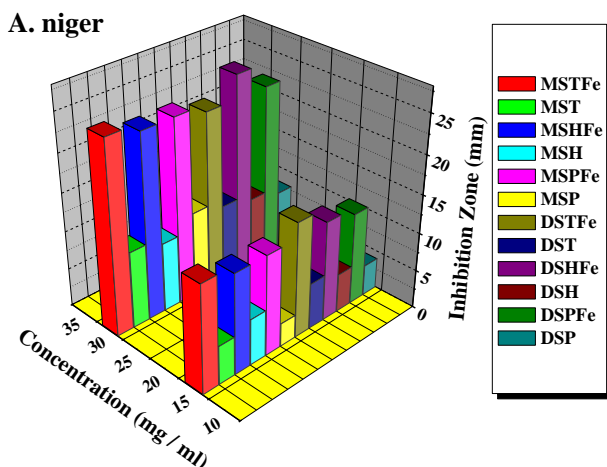


Fig. 9: Antifungal evaluation of the investigated Schiff base amino acid ligands and their complexes against *A. niger* fungi.

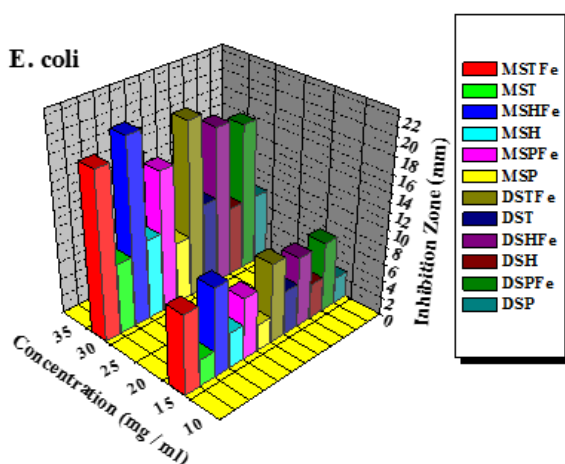


Fig. 10: Antibacterial evaluation of the investigated Schiff base amino acid ligands and their complexes against *E. coli* bacteria.

3.3. DNA binding analysis

Titration by using electronic absorption spectroscopy is an efficient method to explore the binding mode of DNA with a metal complex [50]. If the binding mode is intercalation, the orbital of implanted ligand can couple with the orbital of the base pairs, lowering the $\pi\text{-}\pi^*$ transition energy and consequential in bathochromism. If the coupling orbital is partially filled by electrons, it results in shrinking the transition probabilities and leading to hypochromism [51]. Moreover, addition of increasing amounts of CT-DNA leads to a decrease of absorbance for each investigated complex. In the absence and presence of different concentration of buffered CT-DNA, the electronic absorption spectra of the synthesized

complexes are assumed in Table 6 and Fig. 11. From a comparison between the value of binding constant (K_b) of ethidium bromide, the known DNA intercalator (EB, $K_b = 1.4 \times 10^6 \text{ mol}^{-1}\text{dm}^{-3}$) and the values of the binding constants (K_b) of the prepared Schiff base amino acid complexes, it is found that all the prepared Schiff base amino acid complexes have high values of binding constants (K_b) near to the control (EB). These results promise that these complexes can be used in cancer therapy.

Viscosity measurements were carried out to provide information about binding model between complexes and DNA. The relative specific viscosity of DNA increased, by increasing concentrations of complexes, but the increasing that observed for the typical intercalator ethidium bromide (EB) is higher than that revealed for the prepared complexes, indicating that intercalative as shown in Fig. 12. The intercalation model results in lengthening of the DNA helix as base pairs to rise of DNA viscosity [52].

DNA binding studies are essential for the rational design and composition of new and more efficient drugs targeted to DNA. The cleavage efficiency of complexes was compared to that of the control is due to their effective DNA binding ability. Control experiment using DNA alone does not show any notable cleavage of CT-DNA even on longer exposure time. The variation in DNA-cleavage efficiency of ligands/metal ion complexes was due to their difference in binding ability of ligands/complexes to DNA. The intensity of lanes Fig. 13 was higher in the sequence: $\text{MSTFe} > \text{MSPFe} > \text{MSHFe} > \text{DSPFe} > \text{DSHFe} > \text{DSTFe}$ and these are in a good agreement with binding constant values and viscosity measurements of the synthesized complexes with CT-DNA [53]. It was concluded that as the complexes was observed to split the DNA, therefore reduces the growth of the pathogenic organism by cleaving the genome.

Table 6: Spectral parameters for DNA interaction with the prepared complexes

Complex	λ_{max} free (nm)	λ_{max} bound (nm)	Δn (nm)	Chromism (%) ^a	$10^5 K_b$ $\text{mol}^{-1}\text{dm}^3$	ΔG^\ddagger KJ mol^{-1}
MSPFe	245	243	2	15.9	4.5	-32.4
	500	554	54	48.0		
MSTFe	253	251	2	35.0	5.4	-32.9
	518	522	4	91.9		
MSHFe	249	247	2	21.2	3.6	-31.9
	521	519	2	88.6		
DSPFe	244	245	1	20.5	3.4	-31.8
	511	529	18	82.5		
DSTFe	251	236	15	15.6	0.4	-26.1
	514	532	18	50.0		
DSHFe	247	241	6	17.5	2.5	-31.0
	495	530	65	96.2		

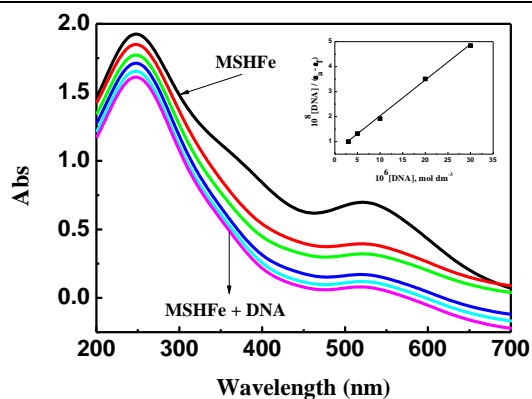


Fig. 11: Spectral scans of the interaction of MSHFe complex (10^{-3} mol dm^{-3}) in 0.01 mol dm^{-3} Tris buffer (pH 7.2, 298 K) with CT – DNA (3-30 μM intervals). Plot of $[\text{DNA}] / (\epsilon_a - \epsilon_f)$ versus $[\text{DNA}]$ for the titration of DNA with MSHFe complex.

3.4. Antioxidant activities of the synthesized complexes

Antioxidant activities of the prepared complexes were determined based on the Trolox calibration curve and expressed in $\mu\text{mol/L}$ of Trolox equivalents ($\mu\text{mol TE/L}$). The radical activity were found 111.64, 55.85, 227.27, 87.72, 41.86 and 56.00 $\mu\text{mol TE/L}$ for complexes of MSTFe, MSPFe, MSHFe, DSTFe, DSPFe and DSHFe respectively. Fig. 14 illustrates the percent inhibition % of radical for the investigated complexes. It is obvious that MSHFe complex shows the strongest potent radical scavenging activity with percent of 72.12 % then MSTFe complex (35.44 %). In conclusion, the complexes exhibit potential antioxidant property and highest activity is observed to MSHFe complex. It is very important to develop compounds with both strong antioxidant and DNA-binding properties for effective cancer therapy.

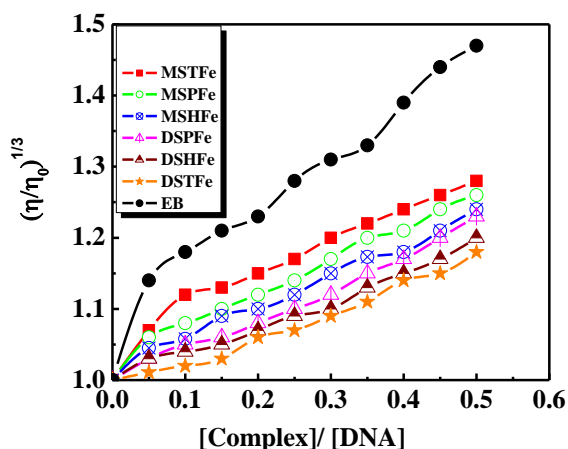


Fig. 12: The effect of increasing concentration of the synthesized complexes on the relative viscosities of DNA at $[\text{DNA}] = 0.5$ μM , $[\text{complex}]$ and $[\text{EB}] = 25\text{-}250$ μM and 298 K.

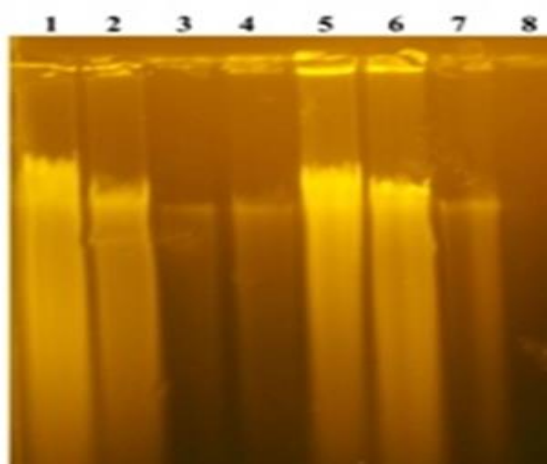


Fig. 13: DNA binding results of the prepared Schiff base amino acid Fe (II) complexes based on gel electrophoresis. Lane 1: CT - DNA, Lane 2: CT – DNA + DSPFe, Lane 3: CT – DNA + MSPFe, Lane 4: CT – DNA + MSHFe, Lane 5: CT – DNA + DSTFe, Lane 6: CT – DNA + DSHFe, Lane 7: DNA + MSTFe and Lane 8: MSTFe.

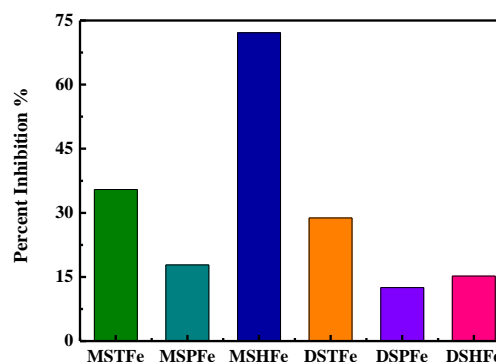


Fig. 14: Radical scavenging activity of the prepared complexes using ABTS radical.

4 Conclusions

In this paper, the newly synthesized Schiff base amino acid ligands act as tridentate ligands coordinating to metal ion by way of phenolic-oxygen atoms, azomethine nitrogen, and carboxylate oxygen atom. Octahedral geometries have been proposed for the prepared Fe (II) complexes with the help of different spectral studies like IR, UV-Vis, $^1\text{H NMR}$, $^{13}\text{C NMR}$ spectra with the general formula $[\text{Fe}(\text{HL})_2] \cdot n\text{H}_2\text{O}$. But in the case of MSHFe complex, the MSH ligand acts as tetradentate $(\text{NH}_4^+)[\text{Fe}(\text{HL})(\text{H}_2\text{O})\text{SO}_4] \cdot 2\text{H}_2\text{O}$. The suggested structures were confirmed by applying the molar ratio and continuous variation methods. Moreover, the obtained formation constants (K_f) values indicate the high stability of the prepared Fe (II) complexes. The particle size distributions of the prepared complexes were found in the range of nanoparticles. The Schiff bases and their metal complexes were found to be active against some of the antibacterial and antifungal species. The activity is

significantly increased on coordination. Furthermore, The DNA interaction study takes intercalative mode. These findings clearly indicate that transition metal-based complexes have many practical applications, like the development of nucleic acid molecular probes and new therapeutic reagents for diseases. The prepared complexes exhibit potential antioxidant property and highest activity is observed to MSHFe complex.

References

- [1] (a) Rekha, S. & Nagasundara, K. R., Complexes of the Schiff base derived from 4-amino-phenyl benzimidazole and 2,2 -dehydroproline-N-aldehyde with Zn(II), Cd(II) and Hg(II) halides, *In. J. Chem.*, 45 (2006) 2424-2425.
- [2] McMenamy, R. H. & Oncley, J. L., The specific binding of L-tryptophan to serum albumin, *J. Biol. Chem.*, 233 (1958) 1436-1447.
- [3] Yuwiler, A., Oldendorf, W. H., Geller, E., Braun, L., Effect of albumin binding and amino acid competition on tryptophan uptake into brain. *J. Neuro. chem.*, 28 (1977) 1015-1023.
- [4] (a) Prendergast, G. C., Chang, M. Y., Mandik-Nayak, L., Metz, R., Muller, A. J., Indoleamine 2,3-dioxygenase as a modifier of pathogenic inflammation in cancer and other inflammation-associated diseases, *Curr. Med. Chem.*, 18 (2011) 2257-2262; (b) Abdel-Rahman, L. H., El-Khatib, R. M., Nassr, L. A. E., Abu-Dief, A. M., DNA binding ability mode, spectroscopic studies, hydrophobicity, and in vitro antibacterial evaluation of some new Fe (II) complexes bearing ONO donors amino acid Schiff bases, *Arabian J. Chem.* 10 (2017) S1835-S1846; (c) Abu-Dief, A. M., Abdel-Rahman, L. H., Abdel-Mawgoud, A. A. H., A robust in vitro anticancer, antioxidant and antimicrobial agents based on new metal-azomethine chelates incorporating Ag (I), Pd (II) and VO (II) cations: Probing the aspects of DNA interaction, *Appl. Organomet. Chem.* 34 (2020) e5373
- [5] (a) You, Z. L., Zhu, H. L., Liu, W. S., Solvothermal Syntheses and Crystal Structures of Three Linear Trinuclear Schiff Base Complexes of Zinc(II) and Cadmium(II), *Z. Anorg. Allg. Chem.*, 630 (2004) 1617-1622; (b) Aljohani, E. T., Shehata, M. R., Abu-Dief, A. M., Design, synthesis, structural inspection of Pd²⁺, VO²⁺, Mn²⁺, and Zn²⁺ chelates incorporating ferrocenyl thiophenol ligand: DNA interaction and pharmaceutical studies *Applied Organometallic Chemistry* 35 (4), 2021, e6169; (c) Abu-Dief, A. M., Abdel-Rahman, L. H., Shehata, M. R., Abdel-Mawgoud, A. A. H., Novel azomethine Pd (II)-and VO (II)-based metallo-pharmaceuticals as anticancer, antimicrobial, and antioxidant agents: Design, structural inspection, DFT investigation, and DNA interaction, *Journal of Physical Organic Chemistry*, 32 (12), (2019) e4009.
- [6] (a) Singh, K., Barwa, M. S., Tyagi, P., Synthesis, characterization and biological studies of Co(II), Ni(II), Cu(II) and Zn(II) complexes with bidentate Schiff bases derived by heterocyclic ketone, *Eur. J. Med. Chem.*, 41 (2006) 147-153; (b) Al-Abdulkarim, H. A., El-khatib, R. M., Aljohani, F. S., Mahran, A., Alharbi, A., Mersal, G. A. M., El-Metwaly, N. M., Abu-Dief, A. M., Optimization for synthesized quinoline-based Cr³⁺, VO²⁺, Zn²⁺ and Pd²⁺ complexes: DNA interaction, biological assay and in-silico treatments for verification, *Journal of Molecular Liquids* 339(2021) 116797; (c) Abu-Dief, A. M., El-Khatib, R. M., Aljohani, F. S., Alzahrani, S. O., Mahran, A., E Khalifa, M., El-Metwaly, N. M., Synthesis and intensive characterization for novel Zn (II), Pd (II), Cr (III) and VO (II)-Schiff base complexes; DNA-interaction, DFT, drug-likeness and molecular docking studies, *Journal of Molecular Structure* 1242, 2021, 130693.
- [7] (a) Majumder, A., Rosair, G. M., Mallick, A., Chattopadhyay, N., Mitra, S., Synthesis, structures and fluorescence of nickel, zinc and cadmium complexes with the N, N, O-tridentate Schiff base N-2-pyridylmethylidene-2-hydroxy-phenylamine, *Polyhedron*, 25 (2006) 1753-1762; (b) Aljohani, E. T., Shehata, M. R., Alkhatib, F., Alzahrani, S. O., Abu-Dief, A. M., Development and structure elucidation of new VO²⁺, Mn²⁺, Zn²⁺, and Pd²⁺ complexes based on azomethine ferrocenyl ligand: DNA interaction, antimicrobial, antioxidant, anticancer activities, and molecular docking *Applied Organometallic Chemistry* 35 (5), 2021, e6154.
- [8] (a) Freiria, A., Bastida, R., Valencia, L., Macias, A., Lodeiro, C., Metal complexes with two tri-aza and tri-oxa pendant-armed macrocyclic ligands: Synthesis, characterization, crystal structures and fluorescence studies, *Inorg.Chim.Acta*, 359 (2006) 2383-2394; (b) Abu-Dief, A. M., El-khatib, R. M., El Sayed, S. M., Alzahrani, S., Alkhatib, F., El-Sarrag, G., Ismael, M., Tailoring, Structural elucidation, DFT calculation, DNA interaction and pharmaceutical applications of some aryl hydrazone Mn (II), Cu (II) and Fe (III) complexes, *Journal of Molecular Structure* 1244 (2021)131017.
- [9] (a) Erkkila, K. E., Odom, D. T., Barton, J. K., Recognition and Reaction of Metallointercalators with DNA, *Chem. Rev.*, 99(1999) 2777-2796; (b) Abu-Dief, A. M., El-Metwaly, N. M., Alzahrani, S. O., Alkhatib, F., Abual-naja, M. M., El-Dabea, T., Ali, M. A. A., Synthesis and characterization of Fe (III), Pd (II) and Cu (II)-thiazole complexes; DFT, pharmacophore modeling, in-vitro assay and DNA

- binding studies, *J. Mol. Liq.* 326 (2021) 115277.
- [10] (a) Vijayalakshmi, R., Kanthimathi, M., Subramanian, V., Nair, B. N., Interaction of DNA with [Cr (Schiff base) (H₂O)₂] ClO₄, *Biochim. Biophys. Acta*, 1475 (2000) 157-162; (b) Abu-Dief, A. M., Abdel-Rahman, L. H., Abdelhamid, A. A., Marzouk, A. A., Shehata, M. R., Bakheet, M. A., Almaghrabi, O. A., Nafady, A., Synthesis and characterization of new Cr (III), Fe (III) and Cu (II) complexes incorporating multi-substituted aryl imidazole ligand: Structural, DFT, DNA binding, and biological implications, *Spectrochim. Acta A* 228 (2020) 117700.
- [11] (a) Wang, X. Y., Zhang, J., Li, K., Jiang, N., Chen, S. Y., Lin, H. H., Huang, Y., Ma, L. J., Yu., X. Q., Synthesis and DNA cleavage activities of mononuclear macrocyclic polyamine zinc(II), copper(II), cobalt(II) complexes which linked with uracil, *Bioorg. Med. Chem.*, 14(2006) 6745-6751; (b) Abdel-Rahman, L. H., Adam, M. S., Abu-Dief, A. M., Moustafa, H., Basha, M., Aboria, A. H., Al-Farhan, B. S., Ahmed, H. E., Synthesis, theoretical investigations, biocidal screening, DNA binding, in vitro cytotoxicity and molecular docking of novel Cu (II), Pd (II) and Ag (I) complexes of chlorobenzylidene Schiff base: Promising antibiotic and anticancer agents, *Appl. Organomet. Chem.* (2018) 32, e4527.
- [12] (a) Raman, N., Raja, J. D., Sakthivel, A., Synthesis, spectral characterization of Schiff base transition metal complexes: DNA cleavage and antimicrobial activity studies, *J. Chem. Sci.*, 119(4) (2007) 303-309; (b) Abdel-Rahman, L. H., Abu-Dief, A. M., Aboelez, M. O., Abdel-Mawgoud, A. A. H., DNA interaction, antimicrobial, anticancer activities and molecular docking study of some new VO (II), Cr (III), Mn (II) and Ni (II) mononuclear chelates encompassing quaridentate imine ligand, *J. Photochem. Photobiol. B*, 170(2017) 271
- [13] (a) Begum, M. S. A., Saha, S., Nethaji, M., Chkravarty, A. R., Iron (III) Schiff base complexes of arginine and lysine as netropsin mimics showing AT-selective DNA binding and photonuclease activity, *J. Inorg. Biochem.*, 104(2010) 477-484; (b) Abdel-Rahman, L. H., Abu-Dief, A. M., Mostafa, H., Hamdan, S. K., *Appl. Organomet. Chem.* 31(2017) e3555.
- [14] Goldberg, D. E., Sharma, V., Oksman, A., Gluzman, I. Y., Probing the chloroquine resistance locus of *Plasmodium falciparum* with a novel class of multidentate metal (III) coordination complexes, *J. Biol. Chem.*, (1997) 272.
- [15] Sakiyan, I., Logoglu, E., Arslan, S., Sari, N., Sahiyan, N., *BioMetals*, 17(2) (2004) 115-120.
- A. Abu-Deif *et al.*: Structure explication, biological...
- [16] Shaker, A. M., Awad, A. M., Nassr, L. A. E., Synthesis and Characterization of Some Novel Amino Acid Schiff Base Fe(II) Complexes, *Synth. Inorg. Metal-Org. Chem.*, 33(1) (2003) 103.
- [17] (a) El-Sharief, A. M. S., Ammar, M. S., Ammar, Y. A., Zak, M. E., *Ind. J. Chem.*, 22 B (1983) 700-704; (b) El-Remaily, M. A., El-Dabea, T., Alsawat, M., Mahmoud, M. H. H., Alfi, A. A., El-Metwaly, N., Abu-Dief, A. M., Development of new thiazole complexes as powerful catalysts for synthesis of pyrazole-4-carbonitrile derivatives under ultrasonic irradiation condition supported by DFT studies, *ACS omega* 6 (32), 2021, 21071-21086.
- [18] Pelczar, M. J., Chan, E. C. S., Kreig, N. R., Antibiotics and other chemotherapeutic agents. In: D. D. Edwards, M. F. Pelczar, editors. *Microbiology: Concepts and applications*, 6th ed., New York: McGraw-Hill Inc; (1993) 556-88; (b) Abdel-Rahman, L. H., El-Khatib, R. M., Nassr, L. A. E., Abu-Dief, A. M., Ismael, M., Metal based pharmacologically active agents: synthesis, structural characterization, molecular modeling, CT-DNA binding studies and in vitro antimicrobial screening of iron (II) bromosalicylidene amino acid chelates, *Spectrochim. Acta A*, 117 (2014) 366; (c) Abdel-Rahman, L. H., Abu-Dief, A. M., Ismail, N. M., Ismael, M., Synthesis, characterization, and biological activity of new mixed ligand transition metal complexes of glutamine, glutaric, and glutamic acid with nitrogen based ligands, *Inorg. Nano-Metal Chem.* 2017, 47, 467.
- [19] (a) Sirajuddin, M., Ali, S., Haider, A., Shah, N. A. A., Shah, Khan, M. R., Synthesis, characterization, biological screenings and interaction with calf thymus DNA as well as electrochemical studies of adducts formed by azomethine [2-((3, 5-dimethylphenylimino)m, *Polyhedron*, 40(2012) 19-31; (b) Abdel-Rahman, L. H., Abu-Dief, A. M., El-Khatib, R. M., Abdel-Fatah, S. M., Some new nano-sized Fe (II), Cd (II) and Zn (II) Schiff base complexes as precursor for metal oxides: Sonochemical synthesis, characterization, DNA interaction, in vitro antimicrobial and anticancer activities, *Bioorg. Chem.*, 69 (2016) 140; (c) Abdel-Rahman, L. H., Abu-Dief, A. M., El-Khatib, R. M., Abdel-Fatah, S. M., Sonochemical synthesis, DNA binding, antimicrobial evaluation and in vitro anticancer activity of three new nano-sized Cu (II), Co (II) and Ni (II) chelates based on tri-dentate NOO imine ligands as precursors for metal oxides. *Journal of Photochemistry and Photobiology B: Biology* 162, 298-308.
- [20] (a) Satyanarayana, S., Dabrowiak, J. C., Chaires, J. B., Tris (phenanthroline) ruthenium (II) enantiomer interactions with DNA: mode and specificity of

- binding, *Biochem.*, 32 (1993) 2573-2584; (b) Abdel Rahman, L. H., Abu-Dief A. M., El-Khatib R. M., Abdel-Fatah, S. M., Sonochemical synthesis, spectroscopic characterization, 3d molecular modeling, DNA binding and antimicrobial evaluation of some transition metal complexes based on bidentate no donor imine ligand, *International Journal of Nanomaterials and Chemistry* 4 (1) (2018) 1-17.
- [21] Lee, P. Y., Costumbrado, J., Chih-Yuan Hsu, Kim, Y. H., Agarose Gel Electrophoresis for the Separation of DNA Fragments, *The Journal of Visualized Experiments*, 62(2012)PMID 22546956.
- [22]"Agarose gel electrophoresis (basic method)", *Biological Protocols*, Retrieved 23 August 2011.
- [23] Villano, D., Fernandez-Pachon, M. S., Troncoso, A. M., Garcia-Parrilla, M. C., The antioxidant activity of wines determined by the ABTS+ method: Influence of sample dilution and time, *Talanta*, 64 (2004) 501-509.
- [24] Salavati-Niasari, M., Salimi, Z., Bazarganipour, M., Davar, F., Inorg. Synthesis, characterization and catalytic oxidation of cyclohexane using a novel host (zeolite-Y)/guest (binuclear transition metal complexes) nanocomposite materials, *Chim. Acta*, 362 (2009) 3715-3724.
- [25] Mohanan, K., Aswathy, R., Nitha, L. P., Mathews, N. E., SindhuKumari, B., Synthesis, spectroscopic characterization, DNA cleavage and antibacterial studies of a novel tridentate Schiff base and some lanthanide(III) complexes, *J. rare earths*, 32(4) (2014) 379-388.
- [26] Lekha, L., Raja K. K., Rajagopal, G., Easwaramoorthy D., Schiff base complexes of rare earth metal ions: Synthesis, characterization and catalytic activity for the oxidation of aniline and substituted anilines, *J. Organomet. Chem.*, 753 (2014) 72-80.
- [27] Ajlouni, A. M., Taha, Z. A., Momani, W. A., Hijazi, A. K., Ebqa'ai, M., Synthesis, characterization, biological activities, and luminescent properties of lanthanide complexes with N, N'-bis (2-hydroxy-1-naphthylidene)-1, 6-hexadiimine, *Inorg. Chim. Acta*, 388 (2012) 120.
- [28] Singh, K., Kumar, Y., Pundir, R. K., Synthesis and Characterization of biologically active organosilicon (IV) complexes with Schiff bases derived from o-aminothiophenol, *Synthesis and Reactivity in Inorganic and Metal-Organic Chemistry*, 40 (2010) 836-842.
- [29] Nath, M., Saini, P. K., Kumar, A., New di-and triorganotin(IV) complexes of tripodal Schiff base ligand containing three imidazole arms: Synthesis, structural characterization, anti-inflammatory activity and thermal studies, *J. Organomet. Chem.*, 695 (2010) 1353-1362.
- [30] (a) Ferrero, J. R., Low-frequency vibrations of inorganic and coordination compounds, John Wiley & Sons, New York, (1971); (b) Abdel-Rahman, L. H., Abu-Dief, A. M., Adam M. S. S., Hamdan, S. K., Some New Nano-sized Mononuclear Cu(II) Schiff Base Complexes: Design, Characterization, Molecular Modeling and Catalytic Potentials in Benzyl Alcohol Oxidation, *Catalysis Letters* 146, (2016) 1373-1396.
- [31] (a) Singh, H. L., Varshney, A. K., Synthesis and characterization of coordination compounds of organotin (IV) with nitrogen and sulphur donor ligands, *Appl. Organomet. Chem.*, 15 (2001) 762-768; (b) Abdel-Rahman, L. H., Abu-Dief, A. M., Atlam F. M., Abdel-Mawgoud, A. A. H., Alotman, A. A., Alsalme A. M., Nafady, A., Chemical, physical and biological properties of Pd(II), V(IV)O, and Ag(I) complexes of N³ tridentate pyridine based Schiff base ligand, *Journal of Coordination Chemistry* 73 (23), (2020) 3150-3173.
- [32] Kalia, S. B., Lumba, K., Kaushal, G., Sharma, M., Magnetic and spectral studies on Co(II) chelates of a dithiocarbamate derived from isoniazid, *Ind. J. Chem.*, 46 A (2007) 1233-1239, V. Philip, V. Suni, M. R. P. Kurup, M. Nethaji, *Polyhedron*, 23 (2004) 1225-1233.
- [33] Ghosh, S., Cirera, J., Vance, M. A., Ono, T., Fujisawa, K., Solomon, E. I., Spectroscopic and electronic structure studies of phenolate Cu (II) complexes: phenolate ring orientation and activation related to cofactor biogenesis, *J. Am. Ch. Soc.*, 130(48) (2008) 16262-16273.
- [34] Nardo, J. V., Dawson, J. H., Spectroscopic Evidence for the Coordination of Oxygen Donor Ligands to Tetraphenylporphinatozinc, *Inorg. Chem. Acta*, 123 (1986) 9-13.
- [35] Maurya, M. R., Gopinathan, C., Synthesis and characterization of dioxotungsten (VI) and dioxomolybdenum (VI) complexes of N-isonicotinamido-o-hydroxyacetophenoneimine via their oxoperoxo complexes, *In. J. Chem., A: Inorg. Phys. Theor. Anal. Chem.*, 35(8) (1996) 701-703.
- [36] Viroopakshappa, J., Rao, D. V., Synthesis and characterization of cobalt(II), nickel(II) and copper(II) chelates of hydroxy-5-chlorobenzylideneamino)-5-methylisoxazole and hydroxy-5-bromobenzylideneamino)-5-methylisoxazole, *J. In. Chem. Soc.*, 73 (10) (1996) 531-535.

- [37] Mohamed, G. G., Omar, M. M., Hindy, A. M. M., Synthesis, characterization and biological activity of some transition metals with Schiff base derived from 2-thiophene carboxaldehyde and aminobenzoic acid, *Spectrochim. Acta A: Molecular and Biomolecular Spectroscopy*, 62 (4-5)(2005) 1140-1150.
- [38] Aswar, A. S., Bansod, A. D., Aswale, S. R., Mandlik, P. R., Lage, C., Costa-Filho, A. J., Synthesis, characterization, electrical and biological studies of Cr(III), Mn(III), Fe(III), Ti(III), VO(IV), Th(IV), Zr(IV) and UO₂(VI) polychelates with bis-bidentate Schiff base, *In. J. Chem. A*, 43 (2004) 1892-1896.
- [39] Nakamoto, K., *Infrared and Raman Spectra of Inorganic Coordination Compounds*, 3rd ed., New York: J. Wiley and sons (1986).
- [40] (a) Zhang, X. Y., Zhang, Y. J., Yang, L., Yange, R. N., Jin, D. M., Synthesis and characterization of glycine Schiff base complexes of the light lanthanide elements, *Synth. React. Inorg. Met. Org. Chem.*, 30 (2000) 45; (b) Rahman, L. H. A., Abdelhamid, A. A., Abu-Dief, A. M., Shehata, M. R., Bakheet, M. A., Facile synthesis, X-Ray structure of new multi-substituted aryl imidazole ligand, biological screening and DNA binding of its Cr (III), Fe (III) and Cu (II) coordination compounds as potential antibiotic and anticancer drugs, *Journal of Molecular Structure* 1200 (2020) 127034
- [41] Lever, A. B. P., *Inorganic Electronic Spectroscopy*, 298, Elsevier Publishing, Amsterdam, 1968.
- [42] Douglas, S., Donald, W., Holler, F., Crouch, S., *Fundamentals of Analytical Chemistry*, 8th Edition, Saunders College, New York, (2004).
- [43] (a) Hay, P. J., Wadt, W. R., *Ab initio* effective core potentials for molecular calculations. Potentials for the transition metal atoms Sc to Hg, *J. Chem. Phys.*, 82 (1985) 270–283; (b) Abu-Dief, A. M., El-Metwaly, N. M., Alzahrani, S. O., Alkhatib, F., Abumelha, H. M., El-Dabea, T., Ali M. A., Structural, conformational and therapeutic studies on new thiazole complexes: drug-likeness and MOE-simulation assessments, *Research on Chemical Intermediates* 47, (2021) 1979–2002.
- [44] (a) Refat, M. S., El-Sayed, M. Y., Abdel Majid, A., *J. Mol. Stru.*, 1038 (2013) 62–72; (b) Abdel-Rahman, L. H., Abu-Dief, A. M., Moustafa, H., Abdel-Mawgoud, A. A. H., Design and nonlinear optical properties (NLO) using DFT approach of new Cr (III), VO (II), and Ni (II) chelates incorporating tridentate imine ligand for DNA interaction, antimicrobial, anticancer activities and molecular docking studies, *Arabian Journal of Chemistry* 13 (1) (2020) 649-670.
- [45] (a) Mahmoud, W. H., Mohamed, G. G., El-Dessouk, M. M. I., *Spectrochim. Acta Part A: Molecular and Biomolecular Spectroscopy*, 122 (2014) 598–608; (b) Abdel-Rahman, L. H., Adam, M. S. S., Abu-Dief, A. M., Abdel-Mawgoud, A. A. H., Catalytic potential of new mononuclear Cr (III)-Schiff base complexes for selective oxidation of benzyl alcohol by H₂O₂, *Journal of Transition Metal Complexes* 2 (2019) 1-14.
- [46] Belal, A. A. M., El-Deen, I. M., Farid, N. Y., Rosan, Z., Moamen, S. R., *Spectrochim. Acta A: Molecular and Biomolecular Spectroscopy*, 149 (2015) 771–787.
- [47] Abdel-Rahman, L. H., Abu-Dief, A. M., Hashem, N. A., Seleem, A. A., Recent advances in synthesis, characterization and biological activity of nano sized Schiff base amino acid M (II) complexe *Int. J. Nano. Chem.*, 1 (2) (2015) 79-95.
- [48] Abdel-Rahman, L. H., Abu-Dief, A. M., Ismael, M., Mohamed, M. A. A., Hashem, N. A., Synthesis, structure elucidation, biological screening, molecular modeling and DNA binding of some Cu (II) chelates incorporating imines derived from amino acids, *J. Mol. Stru.*, 1103 (2016) 232–244.
- [49] (a) Chaturvedi, K. K., Goyal, M., Antibacterial studies of 7-(α -substituted sulphonamido) methyl- and 7-(α -substituted sulphonamido) phenyl-8-hydroxyquinolines, *J. In. Chem. Soc.*, 61 (1984) 175-176; (b) Abu-Dief, A. M., El-Sagher, H. M., Shehata, M. R., Fabrication, spectroscopic characterization, calf thymus DNA binding investigation, antioxidant and anticancer activities of some antibiotic azomethine Cu (II), Pd (II), Zn (II) and Cr (III) complexes, *Applied Organometallic Chemistry* 33 (8)(2019) e4943; (c) Mohamad, A. D. M., Abualreish, M. A., Abu-Dief, A. M., Temperature and salt effects of the kinetic reactions of substituted 2-pyridylmethylene-8-quinolyl iron (II) complexes as antimicrobial, anticancer and antioxidant agents with Cyanide ions, *Canadian Journal of Chemistry* 99 (9), (2021) 763-772.
- [50] (a) Li, Y., Yang, Z. Y., Wang, M. F., Synthesis, characterization, DNA binding properties, fluorescence studies and antioxidant activity of transition metal complexes with hesperetin-2-hydroxy benzoyl hydrazone, *J. Fluoresc.*, 20 (4) (2010) 891-905; (b) Adam, M. S. S., Abu-Dief, A. M., Makhlof, M. M., Shaaban, S., Alzahrani, S. O., Alkhatib, F., Masaret, G. S., Mohamed, M. A., Alsehli, M., El-Metwaly, N. M., Mohamad, A. D. M, Tailoring, structural inspection of novel oxy and non-oxy metal-imine chelates for DNA interaction, pharmaceutical and molecular docking studies, *Polyhedron* 201 (2021) 115167.

- [51] Sun, Y., Bi, S., Song, D., Qiao, C., Mu, D., Zhang, H., Study of interactions of anthraquinones with DNA using ethidium bromide as a fluorescence probe, *Sensors Actuators B*, 129 (2008) 799-810.
- [52] Vijayalakshmi, R., Kanthimathi, M., Subramanian, V., B.U. Nair, *Biochem, Biophys. Acta*, 1475 (2000) 64-157
- [53] Abdel-Rahman, L. H., El-Khatib, R. M., Nassr, L. A. E., Abu-Dief, A. M., Design, characterization, teratogenicity testing, antibacterial, antifungal and DNA interaction of few high spin Fe (II) Schiff base amino acid complexes, *Spectrochim. Acta A*, 111 (2013) 266-276.